

NJC

Accepted Manuscript



This is an *Accepted Manuscript*, which has been through the Royal Society of Chemistry peer review process and has been accepted for publication.

Accepted Manuscripts are published online shortly after acceptance, before technical editing, formatting and proof reading. Using this free service, authors can make their results available to the community, in citable form, before we publish the edited article. We will replace this *Accepted Manuscript* with the edited and formatted *Advance Article* as soon as it is available.

You can find more information about *Accepted Manuscripts* in the [Information for Authors](#).

Please note that technical editing may introduce minor changes to the text and/or graphics, which may alter content. The journal's standard [Terms & Conditions](#) and the [Ethical guidelines](#) still apply. In no event shall the Royal Society of Chemistry be held responsible for any errors or omissions in this *Accepted Manuscript* or any consequences arising from the use of any information it contains.

Electrical Properties of Organic-Inorganic Hybrid Tin Bromide Cubic Perovskites: Hole-Doping and Iodide Substitution Effects

Hiroyuki Hasegawa* and Tamotsu Inabe*

Received 00th January 20xx,
Accepted 00th January 20xx

DOI: 10.1039/x0xx00000x

www.rsc.org/

Electrical properties of solution-grown organic-inorganic hybrid tin bromide perovskite crystals were evaluated. The resistivity of the as-grown crystal is 10^6 – 10^{10} Ω cm though hole doping of Sn(IV) results in a resistivity decrease by 1–5 orders of magnitude. The activation energy of the semiconducting regime was lower than the one expected on the basis of the band gap. This result suggests that the spontaneous doping as observed for the tin iodide system also occurs for tin bromide, although in this case the acceptor level is separated from the top of the valence band. Iodide substitution effects in tin bromide crystal were investigated using $\text{CH}_3\text{NH}_3\text{SnBr}_{3(1-x)}\text{I}_x$ ($0 \leq x \leq 1$) crystals with variable bromide/iodide ratio. The room temperature resistivity monotonously decreases with increasing iodide content, x . The behavior and optical properties can be explained by the band model in which iodide substitution lifts up the top of the valence band and makes the energy difference to the acceptor levels smaller. In addition, a negative differential resistance behavior was observed in the bromide-rich region.

Introduction

As highlighted by their application as superconductors and ferroelectrics, perovskites are materials whose properties are controllable by substitution of their component atoms.^{1,2} However, the most attractive materials of this class are oxide perovskites, which generally require energy-consuming processes such as ion implantation in order to modify their electronic structure.³ Consequently, there is a strong need for energy-saving techniques, such as solution processing, for the controllable fabrication of semiconductor materials.

Metal halide perovskites⁴ have been considered as wide-gap semiconductors that are close to insulators. However, they have recently attracted considerable attention as next-generation electronic materials owing to their solubility in most organic solvents and excellent electronic properties, such as high carrier mobility^{5–6}. Significant interest in the investigation of these materials has been particularly fuelled by the recent observation of their excellent performance as solar cells.^{7–15}

We have previously shown that spontaneous doping is the origin of the highly conductive nature of tin iodide organic-inorganic hybrid perovskites.^{16–18} The cubic $\text{CH}_3\text{NH}_3\text{SnI}_3$ perovskite (Figure 1) has a band gap of 1.3 eV; however, the temperature dependence of its electrical conductivity and thermoelectric power is consistent with metallic behavior. The thermoelectric power value also suggests that a small number

of carriers (holes) are doped into the upper edge of the valence band. Furthermore, Hall effect measurements have allowed the doping level to be estimated as 0.02%. On the basis of these results, we concluded that this material is a doped semiconductor.¹⁸ Recently, Kanatzidis *et al.* reported that this crystal can be dedoped using a large excess of a reductant.¹⁹ Accordingly, this crystal has a semiconducting

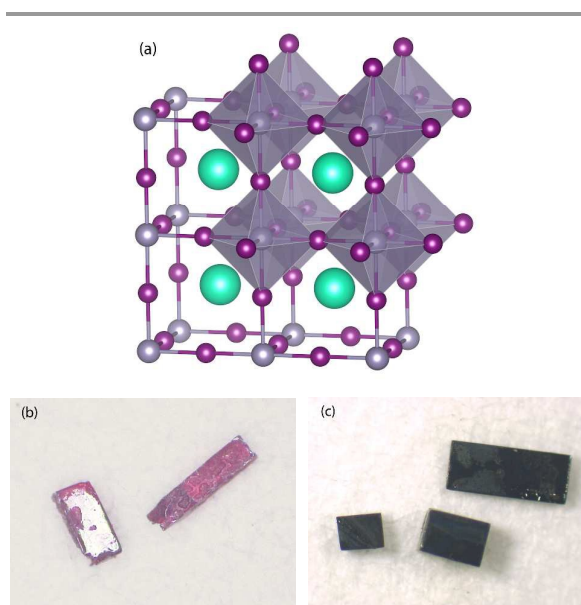


Figure 1. (a) Cubic perovskite structure. A metal atom is located at the center of each octahedron. The green spheres indicate A-sites for cations such as methylammonium. (b) $\text{CH}_3\text{NH}_3\text{SnBr}_3$ and (c) $\text{CH}_3\text{NH}_3\text{SnI}_3$ crystals obtained.

^a Faculty of Science, Hokkaido University, Kita 10 Nishi 8, Kita-ku, Sapporo 060-0810, Japan.

* Corresponding authors: hase@sci.hokudai.ac.jp (H.H.), inabe@sci.hokudai.ac.jp (T.I.).

band structure, though the doping level depends on the sample preparation. Conversely, tin bromide cubic perovskite, $\text{CH}_3\text{NH}_3\text{SnBr}_3$, exhibits a high resistivity of $10^5\text{--}10^6 \Omega \text{ cm}^{20,21}$ and has a larger calculated band gap than the tin iodide system.²¹ Because these perovskites are isomorphous at room temperature, tin-based mixed halide (iodide and bromide) perovskites can be synthesized with any halogen ratio.^{22,23} Here, two chemical modifications of soluble tin bromide organic-inorganic hybrid perovskite, $\text{CH}_3\text{NH}_3\text{SnBr}_3$, are investigated to clarify the effect that altering the electronic structure has on the electrical properties. The first modification involves chemical doping with a different valence atom, namely tin(IV), while the other involves substitution of the halogen species in tin bromide perovskite. In the second case, four compositions have been reported ($\text{CH}_3\text{NH}_3\text{SnI}_3$, $\text{CH}_3\text{NH}_3\text{SnIBr}_2$, $\text{CH}_3\text{NH}_3\text{SnI}_2\text{Br}$, and $\text{CH}_3\text{NH}_3\text{SnBr}_3$) in previous papers that focused on the linear correlation of their cell parameters with composition,²² the stepwise change in their band gap, and their solar cell characteristics.²³ In this study, we focused on transport properties and investigated more finely divided compositions synthesized by a solution-based crystallization. Tin halide perovskites have also attracted considerable attention as lead-free solar cell materials; hence, in the present paper, we investigate the relationship between the electronic structure and electrical properties of this material. The understanding of this effect is of great importance for the design of various electronic devices.

Experimental section

Synthesis

Commercial SnI_2 (99.9%, Kojundo Chemical Lab. Co. Ltd.), SnBr_2 (99.9%, Kojundo Chemical Lab. Co. Ltd.), and SnBr_4 (99%, Aldrich) reagents were obtained and purified by vacuum sublimation. Methylammonium halides (iodide and bromide) were prepared by the reaction of methylamine with the corresponding aqueous hydrohalogenic acid. The crude product obtained was dissolved in a minimal amount of ethanol, and then recrystallized by adding diethyl ether.

As-grown single crystals of $\text{CH}_3\text{NH}_3\text{SnBr}_3$: Anhydrous ethanol was added to SnBr_2 (0.4178 g, 1.5 mmol) and methylammonium bromide (0.1680 g, 1.5 mmol) under an inert atmosphere. After completely dissolving the solids at 65°C , the solution was cooled to 5°C at a rate of $1\text{--}2^\circ\text{C h}^{-1}$. Dark red cube-like crystals of about 1 mm side were obtained (Figure 1(b)).

Artificially doped single crystals of $\text{CH}_3\text{NH}_3\text{SnBr}_3$: Anhydrous ethanol was added to SnBr_2 (0.2924 g, 1.05 mmol), SnBr_4 (0.1972 g, 0.5 mmol), and methyl ammonium (0.1680 g, 1.5 mmol) under an inert atmosphere. After completely dissolving the solids at 65°C , the solution was cooled to 5°C at a rate of $1\text{--}2^\circ\text{C h}^{-1}$. Dark red cube-like crystals exhibiting essentially the same morphology as the as-grown crystals were obtained. There was no detectable difference between the X-ray diffraction data of the artificially doped and as-grown crystals.

Mixed-halide single crystals of $\text{CH}_3\text{NH}_3\text{SnBr}_{3(1-x)}\text{I}_{3x}$: Anhydrous ethanol was added to a stoichiometric mixture of SnI_2 , SnBr_2 , methyl ammonium iodide, and methyl ammonium bromide under an inert atmosphere. After completely dissolving the solids at 65°C , the solution was cooled to 5°C at a rate of $1\text{--}2^\circ\text{C h}^{-1}$. The color of the obtained crystals gradually changed to black with increasing iodide content (Figure 1(c) for $\text{CH}_3\text{NH}_3\text{SnI}_3$).

X-ray crystal structure analysis

X-ray diffraction data were recorded using a Rigaku R-Axis RAPID imaging plate diffractometer with graphite-monochromated Mo $\text{K}\alpha$ radiation. For this, the crystals were directly mounted on a glass capillary, and the lattice parameter of each crystal was determined from room-temperature measurements. Even though the room-temperature crystal system of both $\text{CH}_3\text{NH}_3\text{SnBr}_3$ and $\text{CH}_3\text{NH}_3\text{SnI}_3$ was identified as pseudo-cubic tetragonal in references 19 and 23, here we assigned it as being cubic as per our previous work.¹⁷ The different crystal system assignment does not affect the interpretation of the electronic structure and physical properties. Based on the known linear correlation between composition and lattice parameter,²² we utilized the obtained lattice parameters for the determination of x .

Electronic properties measurements

All electrical transport properties were measured using single crystals with a Keithley 2636A dual source/meter. These instruments were controlled using custom-written software. All measurements were performed using a standard two-probe method under vacuum conditions. A carbon paste (Dotite XC-12, Fujikura Kasei Co. Ltd.) was used to mount two gold wires ($\Phi = 20 \mu\text{m}$; current source) at both ends of a plate crystal such that the cross section of the crystal was covered with the paste. The original thinner (toluene) of the carbon paste was partially evaporated by a stream of N_2 gas, and then tetralin (1,2,3,4-tetrahydronaphthalene) was added to the paste as a thinner.¹⁶ This procedure was performed in air within 5 min, as per our previous reports^{16–18}, and then the sample was immediately transferred to a vacuum chamber.

Results and discussion

Artificial hole doping reveals the extrinsic semiconductor nature of the as-grown tin bromide crystal. Following artificial hole doping of $\text{CH}_3\text{NH}_3\text{SnBr}_3$ by introducing tetravalent tin, darker red crystals than non-doped tin bromide were obtained. In the case when 20% of Sn(II) was substituted by Sn(IV) in the sample preparation solution, the resistivity of the obtained crystal ($10^5\text{--}10^6 \Omega \text{ cm}$) was reduced by 1–5 orders of magnitude compared to that of the as-grown crystal ($10^6\text{--}10^{10} \Omega \text{ cm}$) due to the carrier (hole) doping effect of Sn(IV). This resistivity is also comparable to that of the sample prepared by the fusion method in references 20 and 21. This result suggests that the crystal obtained by the fusion method generated charge carriers, and exhibited lower resistivity. In the low carrier concentration region of extrinsic semiconductors, the

resistivity is very sensitive to the number of dopants.³ It is considered that this is the reason why the resistivity values are dispersed.

The temperature dependence of the resistivity of artificially doped and as-grown crystals shown in Figure 2(a) provides significant information regarding the band structure. Both crystals exhibit similar activation energies of 0.52 and 0.66 eV for the artificially doped and as-grown crystal, respectively. As these values are much lower than those expected from the optical band gap of ca. 2.0 eV, these crystals must possess acceptor levels and injected carriers. Thus, the spontaneous doping effect seen in the tin iodide system^{16–18} was also found for tin bromide. Assuming that the mobility is comparable to that of the tin iodide system, it can be concluded that the carrier concentration in the crystal is much lower ($\ll 1\%$) than the concentration of Sn(IV) in the mother liquor.

The band diagram for the tin bromide system can be summarized as shown in Figure 2(b). From the results of the band calculation,²⁴ the density of states (DOS) in Figure S1 indicates that both the 5s orbital of tin and p orbital of halogen contribute to the upper edge of the valence band, whereas only the 5p orbital of tin contributes to the bottom of the conduction band. When redox potential and electron affinity are taken into account, the energy level of the outer p orbitals of iodine is higher than that of bromine. This factor makes the band gap of tin iodide narrower than that of tin bromide. Furthermore, if the same acceptor level as for tin iodide was

also formed in the tin bromide system, it would be reasonable to expect that the activation energy of the tin bromide system would be larger than that of the tin iodide system. In reality, as the acceptor level in the tin iodide system almost overlaps with the top edge of the valence band, the system exhibits metallic behavior in the temperature dependence of the conductivity. However, since the acceptor level in the tin bromide system is separated by more than 0.5 eV from the top edge of the valence band, semiconducting behavior was observed. This band diagram is also supported by the results of the diffuse reflectance spectra (Figure S2) and is consistent with the results obtained with copper halide layered perovskites.²⁵ Though this interpretation can explain all the results in this study clearly and consistently, it does not agree with ultraviolet photoelectron spectroscopy (UPS) results²³ that suggest a large energy shift at the bottom of the conduction band. It is hoped that further investigation is required to clarify this difference.

Because cubic methylammonium tin bromide and iodide perovskites are isomorphous, the iodide/bromide ratio can be varied arbitrarily. The crystal structure for each mixed crystal in this study was determined by X-ray diffraction, through which we confirmed that the cubic structure was maintained through halogen substitution.

The transport properties of the materials remarkably reflects the effect of iodide substitution. Figure 3 shows the room temperature resistivity of the various iodide-substituted materials. For $x = 0$, a high resistivity in the range of 10^6 – 10^{10} Ω cm was observed, with the exact value depending on the batch of samples as discussed above. Such resistivity dispersion was also observed in the low- x region for the present synthesized materials; however, the degree of dispersion became smaller with increasing the iodide ratio. In Figure 2(b), the activation energy would be expected to become smaller with iodide substitution, and so the number of carriers is considered to be much higher than in the original tin bromide system. Owing to this increase in the number of carriers, the resistivity will become more insensitive to the number of carriers as discussed above. Depending on the compositional change, the

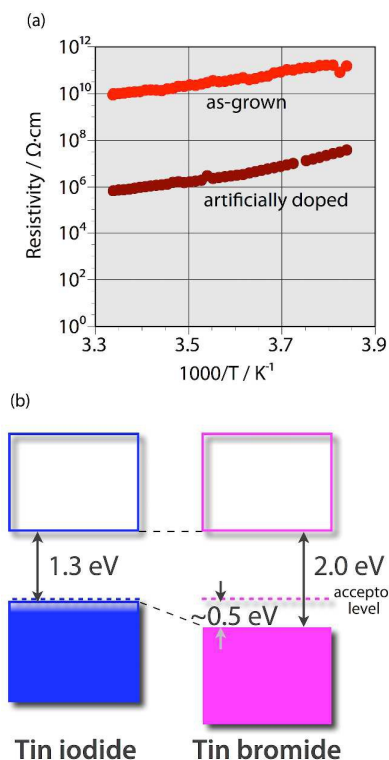


Figure 2. (a) Temperature dependence of the resistivity of the as-grown and the artificially Sn(IV)-doped $\text{CH}_3\text{NH}_3\text{SnBr}_3$ single crystals. (b) Proposed band diagram for the tin iodide and bromide systems in this study.

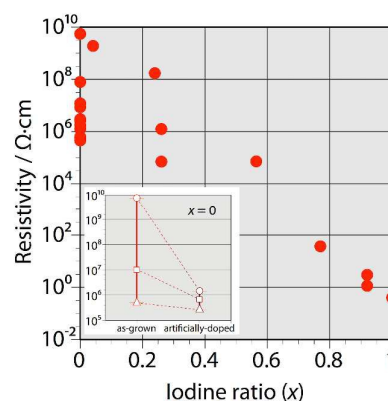


Figure 3. Room temperature resistivity of $\text{CH}_3\text{NH}_3\text{SnBr}_{3(1-x)}\text{I}_3x$ single crystals. Inset represents dispersion of resistivity values for $x = 0$ with as-grown and artificially-doped crystals. Open circles, open squares and open triangles indicate the highest, average and lowest values, respectively.

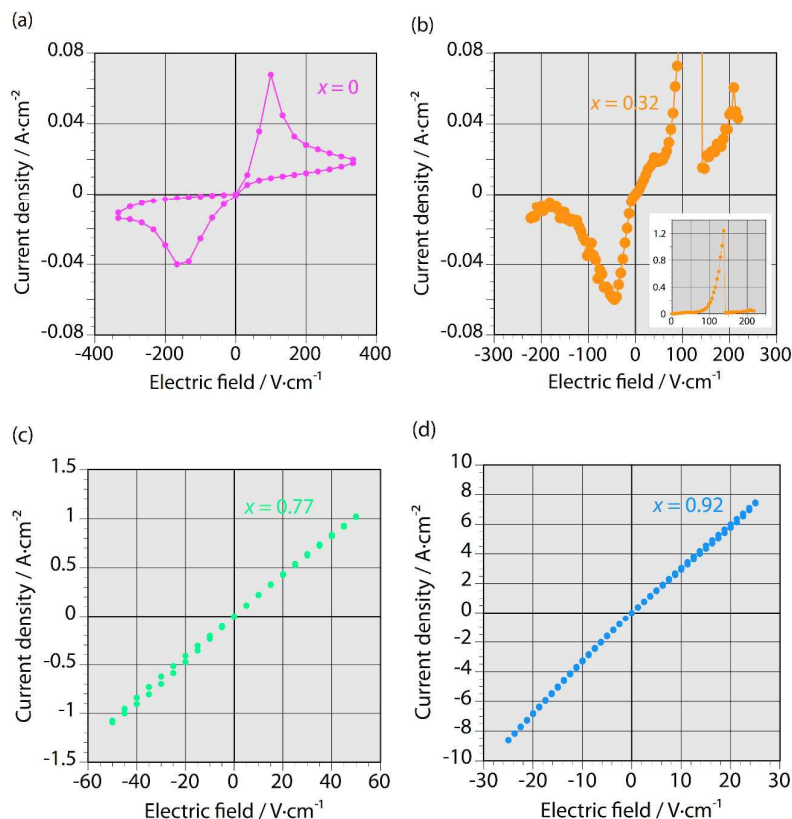


Figure 4. The current density–electric field (J – E) characteristics of $\text{CH}_3\text{NH}_3\text{SnBr}_{3(1-x)}\text{I}_x$ single crystals: (a) $x = 0$, (b) $x = 0.32$, (c) $x = 0.77$, and (d) $x = 0.92$.

resistivity monotonously decreased with increasing iodide content, which is due to the spontaneous doping effect induced by the higher iodide content. As mentioned in the introduction, it is important to note that a spontaneous doping effect is inevitable in the standard procedure used to grow hybrid tin-based perovskite single crystals.

Surprisingly, a negative differential resistance behavior was observed in the bromide-rich region. Figure 4 shows the current density–electric field (J – E) characteristics for some substitution ratios. In the iodide region of $x = 0.77$ and 0.92 , the characteristics denote an ohmic and highly conductive behavior due to the increase number of holes in the valence band of the tin iodide system. On the other hand, as the resistivity increased with decreasing iodide content, non-ohmic characteristics also appeared. Figures 4(a) and (b) show the characteristics measured for $x = 0$ and 0.32 , in which the current density suddenly increased when the electric field reached a specific value, and then decreased with further increase in the electric field. This behavior is typical of negative differential resistance materials. Some binary transition metal oxide perovskites are known to exhibit such resistive switching effect,^{26–30} and so two possibilities can be considered for the present materials. One is the generation of a Schottky barrier junction on one side of the crystal due to an electrochemical reaction inside the crystal near its interface with the electrode. The other is a change in the resistance of the conductive path

in the crystal due to the presence of inhomogeneous domains. When the polarity-independent characteristics that have two maximum values in both positive and negative electric fields are taken into account, the latter can be considered the most plausible mechanism at present. In addition, the non-linear characteristics cause dispersion of the resistivity in the low- x region.

Conclusions

The transport characteristics of the tin bromide system indicate that the spontaneous hole doping effect previously seen in the tin iodide system also occurs in the tin bromide system. Carrier doping was also made possible by introducing tetravalent tin. The band diagram of the tin bromide perovskite was proposed. This model can be explained iodide substitution effects in methylammonium tin bromide cubic perovskite crystals such as a reduction of the band gap and an increase in conductivity. On the other hand, The J – E characteristics of the mixed halide $\text{CH}_3\text{NH}_3\text{SnBr}_{3(1-x)}\text{I}_x$ system showed non-ohmic behavior in the bromide rich region; in particular, a negative differential resistance was observed. Halogen substitution in the $\text{CH}_3\text{NH}_3\text{SnBr}_{3(1-x)}\text{I}_x$ system resulted in the modulation of the band gap and acceptor level, which subsequently led to drastic changes in their electrical properties. The properties of these soluble perovskites are

expected to support the development of photovoltaic cells and resistance random access memory (ReRAM) via eco-friendly processes.

Acknowledgements

This research was supported by the CREST program of the Japan Science and Technology Agency (JST). This work was also supported in part by a Grant-in-Aid for Scientific Research, by the Japan Society for the Promotion of Science (JSPS) KAKENHI, and by the JSPS Core-to-Core Program A, Advanced Research Networks. The authors are grateful to Prof. Makoto Wakeshima and Prof. Yukio Hinatsu at Hokkaido University for their help with the band structure calculation.

Notes and references

- 1 *Perovskites and Related Mixed Oxides*, P. Granger, V. I. Parvulescu, S. Kaliaguine, W. Prellier eds., Wiley-VCH, 2015.
- 2 *Properties and Applications of Perovskite-type Oxides*, L. G. Tejuca, J. L. G. Fierro eds., Marcel Dekker, Inc., 1993.
- 3 S. M. Sze, *Semiconductor Devices: Physics and Technology 2nd ed.*, John Wiley & Sons, 2002, Chs. 3 and 13.
- 4 G. C. Papavassiliou, *Prog. Solid St. Chem.*, 1997, **25**, 125–270.
- 5 D. B. Mitzi, C. A. Feild, Z. Schlesinger and R. B. Laibowitz, *J. Solid State Chem.*, 1995, **114**, 159–163.
- 6 D. B. Mitzi, C. A. Feild, W. T. A. Harrison and A. M. Guloy, *Nature*, 1994, **369**, 467–469.
- 7 A. Kojima, K. Teshima, Y. Shirai and T. Miyasaka, *J. Am. Chem. Soc.*, 2009, **131**, 6050–6051.
- 8 M. M. Lee, J. Teuscher, T. Miyasaka, T. N. Murakami and H. J. Snaith, *Science*, 2012, **338**, 643–647.
- 9 I. Chung, B. Lee, J. He, R. P. H. Chang and M. G. Kanatzidis, *Nature*, 2012, **485**, 486–489.
- 10 E. J. W. Crossland, N. Noel, V. Sivaram, T. Leijtens, J. A. Alexander-Webber and H. J. Snaith, *Nature*, 2013, **495**, 215–219.
- 11 J. Burschka, N. Pellet, S.-J. Moon, R. Humphry-Baker, P. Gao, M. K. Nazeeruddin and M. Grätzel, *Nature*, 2013, **499**, 316–319.
- 12 E. J. W. Crossland, N. Noel, V. Sivaram, T. Leijtens, J. A. Alexander-Webber, H. J. Snaith, *Nature*, 2013, **495**, 215–219.
- 13 M. Liu, M. B. Johnston, H. Snaith, *Nature*, 2013, **501**, 395–398.
- 14 A. Mei, X. Li, L. Liu, Z. Ku, T. Liu, Y. Rong, M. Xu, M. Hu, J. Chen, Y. Yang, M. Grätzel, H. Han, *Science*, 2014, **345**, 295–298.
- 15 N. J. Jeon, J. H. Noh, W. S. Yang, Y. C. Kim, S. Ryu, J. Seo and S. I. Seok, *Nature*, 2015, **517**, 476–480.
- 16 Y. Takahashi, R. Obara, K. Nakagawa, M. Nakano, J. Tokita and T. Inabe, *Chem. Mater.*, 2007, **19**, 6312–6316.
- 17 Y. Takahashi, R. Obara, Z.-Z. Lin, Y. Takahashi, T. Naito, T. Inabe, S. Ishibashi and K. Terakura, *Dalton Trans.*, 2011, **40**, 5563–5568.
- 18 Y. Takahashi, H. Hasegawa, Y. Takahashi and T. Inabe, *J. Solid State Chem.*, 2013, **205**, 39–43.
- 19 C. C. Stoumpos, C. D. Malliakas and M. G. Kanatzidis, *Inorg. Chem.*, 2013, **52**, 9019–9038.
- 20 K. Yamada, H. Kawaguchi, T. Matsui, T. Okuda and S. Ichiba, *Bull. Chem. Soc. Jpn.*, 1990, **63**, 2521–2525.
- 21 F. Chiarella, A. Zappettini and F. Licci, *Phys. Rev. B*, 2008, **77**, 045129.
- 22 K. Yamada, K. Nakada, Y. Takeuchi, K. Nawa and Y. Yamane, *Bull. Chem. Soc. Jpn.*, 2011, **84**, 926–932.
- 23 F. Hao, C. C. Stoumpos, D. H. Cao, R. P. H. Chang and M. G. Kanatzidis, *Nature Photon.*, 2014, **8**, 489–494.
- 24 P. Blaha, K. Schwarz, G. Madsen, D. Kvasnicka and J. Luitz, *WIEN2k*, An Augmented Plane Wave + Local Orbitals Program for Calculating Crystal Properties (Karlheinz Schwarz, Techn. Universität Wien, Austria), 2001. ISBN 3-9501031-1-2.
- 25 G. S. Lorena, H. Hasegawa, Y. Takahashi, J. Harada and T. Inabe, *Chem. Lett.*, 2014, **43**, 1535–1537.
- 26 A. Asamitsu, Y. Tomioka, H. Kuwahara and Y. Tokura, *Nature*, 1997, **388**, 50–52.
- 27 A. Beck, J. G. Bednorz, Ch. Gerber, C. Rossel and D. Widmer, *Appl. Phys. Lett.*, 2000, **77**, 139–141.
- 28 G. I. Meijer, U. Staub, M. Janousch, S. L. Johnson, B. Delley and T. Neisius, *Phys. Rev. B*, 2005, **72**, 155102.
- 29 K. Shono, H. Kawano, T. Yokota and M. Gomi, *Appl. Phys. Exp.*, 2008, **1**, 055002.
- 30 H. Akinaga and H. Shima, *Proc. IEEE*, 2010, **98**, 2237–2251.

Graphical Abstract for
Electrical Properties of Organic-Inorganic Hybrid Tin Bromide Cubic Perovskites:
Hole-Doping and Iodide Substitution Effects

Hiroyuki Hasegawa* and Tamotsu Inabe*

The spontaneous doping also occurs in tin bromide perovskites. We also found negative differential resistance in bromide-rich mixed halide perovskites.

